

The dynamic effect of pipe-wall viscoelasticity in hydraulic transients. Part I—experimental analysis and creep characterization

L'effet dynamique de la viscoélasticité de la conduite en régimes transitoires hydrauliques. Partie I—analyse expérimental et caractérisation du fluage

DÍDIA COVAS, *Civil Engineering Department, Instituto Superior Técnico, Av. Rovisco Pais, 1049-001 Lisbon, Portugal. E-mail: didia.covas@civil.ist.utl.pt (author for correspondence)*

IVAN STOIANOV, *Civil and Environmental Engineering Department, Imperial College of Science, Technology and Medicine, Imperial College Road, SW7 2BU, London, UK. E-mail: ivan.stoianov@ic.ac.uk*

JOÃO F. MANO, *Polymer Engineering Department, Minho University, Azurém Campus, 4800-058 Guimarães, Portugal. E-mail: jmano@dep.uminho.pt*

HELENA RAMOS, *Civil Engineering Department, Instituto Superior Técnico, Av. Rovisco Pais, 1049-001 Lisbon, Portugal. E-mail: helena.ramos@civil.ist.utl.pt*

NIGEL GRAHAM, *Civil and Environmental Engineering Department, Imperial College of Science, Technology and Medicine, Imperial College Road, SW7 2BU, London, UK. E-mail: n.graham@ic.ac.uk*

CEDO MAKSIMOVIC, *Civil and Environmental Engineering Department, Imperial College of Science, Technology and Medicine, Imperial College Road, SW7 2BU, London, UK. E-mail: c.maksimovic@ic.ac.uk*

ABSTRACT

The mechanical behaviour of the pipe material determines the pressure response of a fluid system during the occurrence of transient events. In viscoelastic pipes, typically made of polyethylene (PE), maximum or minimum transient pressures are rapidly attenuated and the overall pressure wave is delayed in time. This is a result of the retarded deformation of the pipe-wall. This effect has been observed in transient data collected in a high-density PE pipe-rig, at Imperial College (London, UK). Several transient tests were carried out to collect pressure and circumferential strain data. The pipe material presented a typical viscoelastic mechanical behaviour with a sudden pressure drop immediately after the fast valve closure, a major dissipation and dispersion of the pressure wave, and transient mechanical hysteresis. The creep-function of the pipe material was experimentally determined by creep tests, and, its order-of-magnitude was estimated based on pressure-strain data collected from the pipe-rig. A good agreement between the creep functions was observed. Creep tests are important for the characterization of the viscoelastic behaviour of PE as a material; however, when PE is integrated in a pipe system, mechanical tests only provide an estimate of the actual mechanical behaviour of the pipe system. This is because creep depends on not only the molecular structure of the material and temperature but also on pipe axial and circumferential constraints and the stress-time history of the pipe system.

RÉSUMÉ

En régime transitoire, les variations de pression dans un système de type fluide sont déterminées par la nature du matériau constituant les conduites du système. Dans le cas des conduites viscoélastiques, le plus souvent faites de polyéthylène (PE), les fluctuations de pressions sont atténuées rapidement et l'onde de pression est retardée, à cause du délai dans la déformation des parois de la conduite. Ce phénomène a été observé à partir de travaux réalisés sur des conduites expérimentales en polyéthylène de haute densité, à l'Imperial College (Londres, Royaume Uni). Divers tests expérimentaux ont été effectués, mesurant la pression et l'extension de la circonférence de la conduite en régime transitoire. Le matériau de la conduite présente un comportement mécanique typiquement viscoélastique caractérisé par une chute de pression immédiatement après la fermeture rapide de la valve, une grande dissipation et dispersion de l'onde de pression, et la présence de boucles (hystérosis) au niveau des courbes de déformation. Le fluage du matériau de la conduite a été évalué expérimentalement par des tests mécaniques, et son ordre de grandeur a été estimé à partir des résultats de pression-extension mesurés directement sur l'installation expérimentale. Une bonne corrélation entre les fonctions de fluage a été observée. Les tests mécaniques de fluage sont importants pour la caractérisation du comportement viscoélastique du PE. Cependant, lorsque le PE est intégré dans un système de conduites, ces tests ne sont pas représentatifs du comportement réel de la conduite, car le fluage dépend non seulement de la structure moléculaire du matériau et de la température, mais aussi des contraintes du système et du passé de la conduite en terme de pressions et de tensions.

Keywords: Hydraulic transients, polyethylene, viscoelasticity, creep, pipe.

Revision received December 4, 2003 / Open for discussion until February 28, 2005.

1 Introduction

In recent years, the use of plastic materials, such as polyethylene (PE) and polyvinyl chloride (PVC), in pipe systems for public and industrial water supply and sewage transport has been gradually increasing throughout the world. This trend reflects a growing confidence in polymers as a pipe material for their excellent mechanical and chemical characteristics, processability, easy and fast assembly and, above all, competitive price. Polymers, in general, exhibit a viscoelastic rheological behaviour (Ferry, 1970; Aklonis *et al.*, 1972; Riande *et al.*, 2000). This behaviour has a significant influence on the mechanical performance of polymers during their lifetime. For example, high density polyethylene (HDPE) may have a short-term modulus of elasticity of 1 GPa and a long-term modulus of 0.7 GPa (Janson, 1995). This time-dependent behaviour is not usually properly accounted for during the design stage of water pipe systems, particularly, with respect to hydraulic transients.

The viscoelastic behaviour is usually manifested by a strain that "lags behind" an applied stress, as the material does not respond instantaneously to an applied load. This behaviour is characterized by an instantaneous elastic strain followed by a gradual retarded strain. In pipe systems, the pipe-wall viscoelasticity influences the pressure response during the occurrence of transient events by causing a mechanical damping of the pressure wave. Pressure fluctuations in pipes are rapidly attenuated, and the pressure wave is delayed in time. This effect has been experimentally observed by several researchers (Fox and Stepnewski, 1974; MeiBner and Franke, 1977; Williams, 1977; Mitosek and Roszkowski, 1998). These authors verified that, in PE pipes, the mechanical damping of the pressure wave during transients, even when the pipe is restrained from moving, is much higher than the viscous damping due to fluid friction. Several other authors proposed mathematical models to describe the viscoelasticity of pipe-wall during fluid transients (Gally *et al.*, 1979; Rieutord and Blanchard, 1979; Rieutord, 1982; Franke and Seyler, 1983; Suo and Wylie, 1990; Covas, 2003; Covas *et al.*, 2002b, 2004a, 2004b).

The current paper is the first of two papers that investigate the effect of the pipe-wall viscoelasticity in fluid transients. Whilst the aim of this paper is the experimental analysis and characterization of the viscoelastic behaviour, the companion paper focuses on the mathematical modelling of the phenomenon during transient events. This analysis is based on an experimental programme carried out at Imperial College (London, UK) with a 277 m HDPE pipeline. Experimental tests were run for different flow regimes collecting both pressure and circumferential strain data. Pipe-wall viscoelasticity is observed in pressure and strain time variations as well as in the stress-strain curves during transient events. This behaviour is characterized by a creep function, which was determined by creep tests carried out at Minho University (Portugal) and Imperial College (UK). The order of magnitude of this creep function was also estimated based on data collected from the pipe-rig and on the calibration of a mathematical model developed in the companion paper Covas *et al.* (2004a). Results of the analysis are discussed and final remarks

are made on how to characterize the viscoelastic behaviour of PE, as a material, and when integrated in a real pipe system.

2 Transient data collection and analysis

2.1 Experimental facility

An experimental facility with a single pipeline system was assembled at the Department of Civil and Environmental Engineering, Imperial College London (Covas *et al.*, 2001, 2002b, 2003a). This facility was designed for the analysis and testing of novel leak detection techniques based on the generation of transient events in the fluid system (Covas *et al.*, 2002a, 2003a; Stoianov *et al.*, 2002). Polyethylene was the chosen pipe material for its low wave speed, high-pressure class, easy assembly and low price. Given the viscoelastic nature of PE, the facility was used to collect pressure and strain data for the analysis of the mechanical behaviour of the pipe, as well as for the calibration and validation of the hydraulic transient solver developed in the companion paper (Covas *et al.*, 2004a).

The pipeline is made of high-density polyethylene SDR11 PE100 NP16, with 63 mm nominal diameter (ND) and 6.2 mm wall thickness. The total length of the pipeline is 271.5 m (length between the vessel and the downstream globe valve). Pipe sections are electrofused and rigidly fixed to a vertical wall with plastic brackets, 1 m spaced along its length, and with metal frames at the elbows, to restrain the pipe from any axial movement. The pipe-rig includes a centrifugal pump ($Q_0 = 2.51/\text{s}$; $H_0 = 35\text{ m}$) and a pressurized tank with 750 l volume, at the upstream end, and a globe valve to control the flow and to generate transient events, at the downstream end. The globe valve discharges directly to a free surface flow drainage pipe. The steady-state flow is measured with an electromagnetic flow meter located immediately after the pressure vessel at the upstream end. The rig configuration is presented in Fig. 1.

The data acquisition system is composed of an acquisition board, eight strain-gauge type pressure transducers (T), four strain gauges (SG) and a notebook computer. The acquisition board has eight analog inputs channels and a maximum sampling rate of 9600 Hz per channel. Pressure transducers have pressure ranges of 0–10 bar (absolute pressure) and an accuracy of 0.3% of the full range. Strain gauges have one single grid, 1 cm length and an electric resistance of $350\ \Omega$ with a class of accuracy $\pm 0.2\%$.

2.2 Data collection

Various data sets were collected with a sampling rate of 600 Hz. Since the acquisition board only allowed eight simultaneous measurements, two sets of experimental tests were run. The first set focused on the collection of pressure data at the eight pipe sections (Locations 1–8). In the second set, pressure and circumferential strain data were collected at three different locations (Locations 1, 5 and 8) and pressure was also monitored at the upstream end (Location 3). Figure 1 shows the location and distance from the upstream end of the measurement sites. Strain gauges were installed in the circumferential direction of the pipe to measure

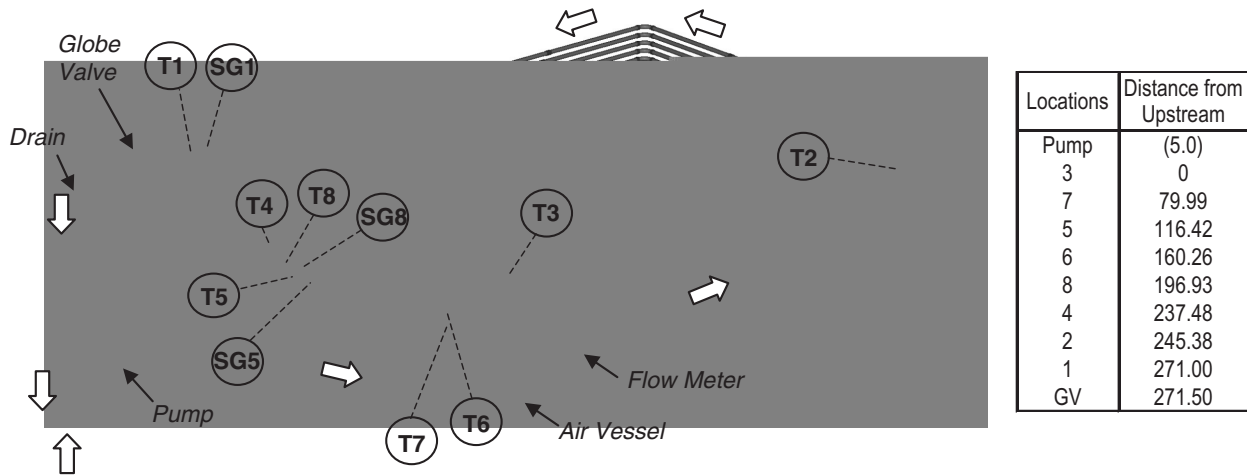


Figure 1 Imperial College experimental facility.

the radial displacement of the pipe cross-section. The axial strain was not measured because the pipe was restrained from moving axially and, in these circumstances, axial strain is negligible compared to the circumferential strain (Gally *et al.*, 1979; Larson and Jonsson, 1991). Transient tests were run for a wide range of steady-state flows from laminar ($Q_0 = 0.05 \text{ l/s}$; $Re = 1,400$) to a smooth-walled pipe flow ($Q_0 = 2.01 \text{ l/s}$; $Re = 50,000$). Transient events were generated by a fast manoeuvre of the globe valve. Closure and opening times varied between 0.06 and 0.20 s.

During the experimental programme, several problems related to data collection were encountered, some of which were overcome or others which were inherent of the mechanical behaviour of the pipe material (Covas *et al.*, 2001). Three main problems are briefly referred herein. The first was associated with pressure oscillations during steady-state conditions. These were caused by cavitation in the flow control valve, initially a gate valve. The problem was resolved by replacing this valve by the current globe valve. The second was the initial spikes in pressure signal immediately after the valve closure. These spikes tended to disappear after the inversion of the first pressure wave. These were due to the mechanical vibration of the waterhammer valve immediately after closure, initially a spherical valve. Several valve configurations at downstream were tested to eliminate the initial spikes that were significantly reduced using the globe valve to generate the waterhammer event. The third problem was related with the sudden pressure drop after closure and the overall pressure damping in consecutive pressure waves. These were initially thought to be related to secondary flow at the elbows that induce flow separation, energy dissipation and secondary reflected waves. Initial short radius elbows (radius 1.5 times ND) were replaced by the current long radius curves (radius five times ND), and compression fittings used to connect pipes were replaced by electrofusion couplers. No difference in the transient pressures was observed after the changes in the pipeline: the initial pressure drop and overall damping and shape of the pressure wave persisted as these were not caused by the elbows but by the non-elastic mechanical behaviour of the pipe. Elbows are completely restrained from moving, thus the wave reflection is negligible. The viscoelastic behaviour of the pipe material is predominant over any other effect, dissipating any small-amplitude high-frequency

oscillation that may occur, such as elbows reflection or valve mechanical vibration.

2.3 Pressure data and wave speed

Transient data collected at Location 1 (Transducer T1) for several steady-state flows are presented in Fig. 2. These data are represented in terms of overpressure, i.e. $\Delta H = p - p_0$ (where p is the transient pressure and p_0 is the steady-state pressure), for several initial flow regimes (from laminar $Q_0 = 0.05 \text{ l/s}$ to smooth-walled pipe flow $Q_0 = 2.01 \text{ l/s}$). Maximum overpressures calculated by the classic Joukovsky formula ($\Delta H = a_0 Q_0 / g S$) using wave speed a_0 estimated based on the static pipe modulus of elasticity, are 10–25% lower than observed overpressures. This is because the static modulus of elasticity of a HDPE pipe varies between 0.7 and 1.0 GPa (according to manufacturers) and the corresponding wave speeds are 280 and 330 m/s (using typical wave speed formulae for thick wall pipes). For the flow of 2.01/s, fast transient events with these wave speeds induce overpressures of 28 and 33.5 m, respectively, whereas the maximum observed overpressure is 37 m (neglecting the line packing effect). Consideration of the line packing effect (Wylie and Streeter, 1993), as it represents an increase of 5–10% of the maximum overpressures, tends to reduce these differences. The underestimation of maximum transient pressures, particularly when using simplified formulae, is an important reason for taking into account the viscoelastic behaviour of PE during transient events.

Transient data collected in the first set of tests at eight pressure transducers for a steady-state flow Q_0 of 1 l/s are presented in Fig. 3(a). The transient event was generated by the closure of the globe valve, starting at $t = 0.2 \text{ s}$. Major energy dissipation is observed accompanied by a phase shift (dispersion) of the pressure wave at all the measurement sites. This phenomenon cannot be completely explained by frictional damping, as this has never been observed with such intensity in metal pipes (Ramos *et al.*, 2004). The excessive dissipation and dispersion are mainly caused by the mechanical damping of the pipe as a result of a retarded deformation of the pipe material that does not respond immediately to an instantaneous pressure load. This is the typical

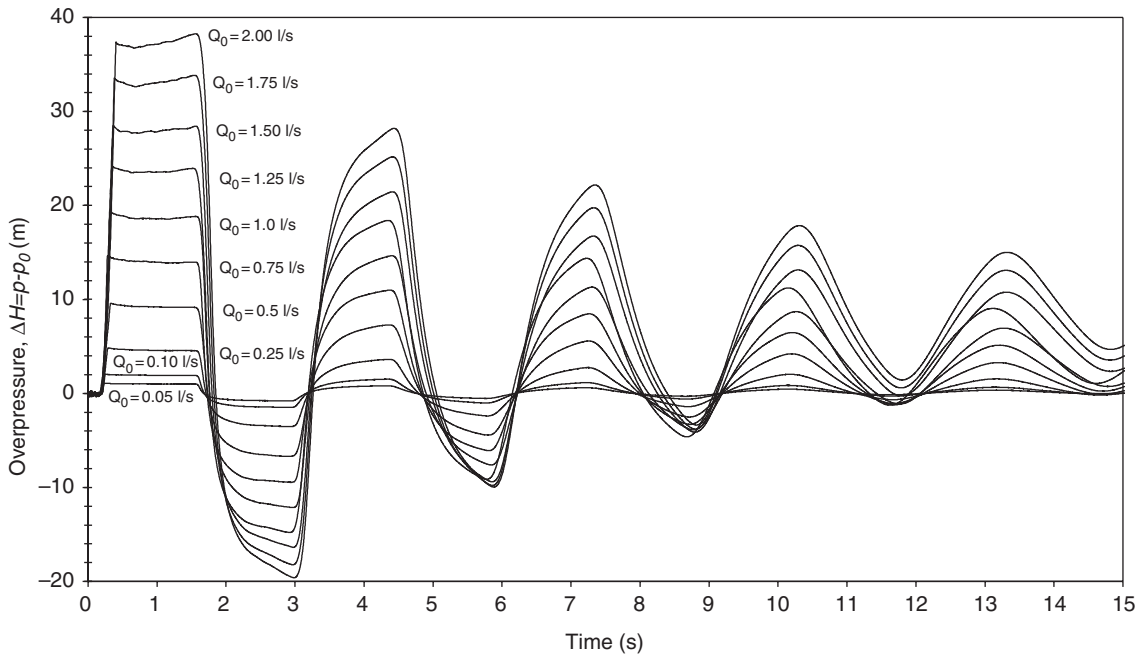


Figure 2 Overpressure at Location 1 generated by the downstream valve closure for several initial steady-state flows Q_0 .

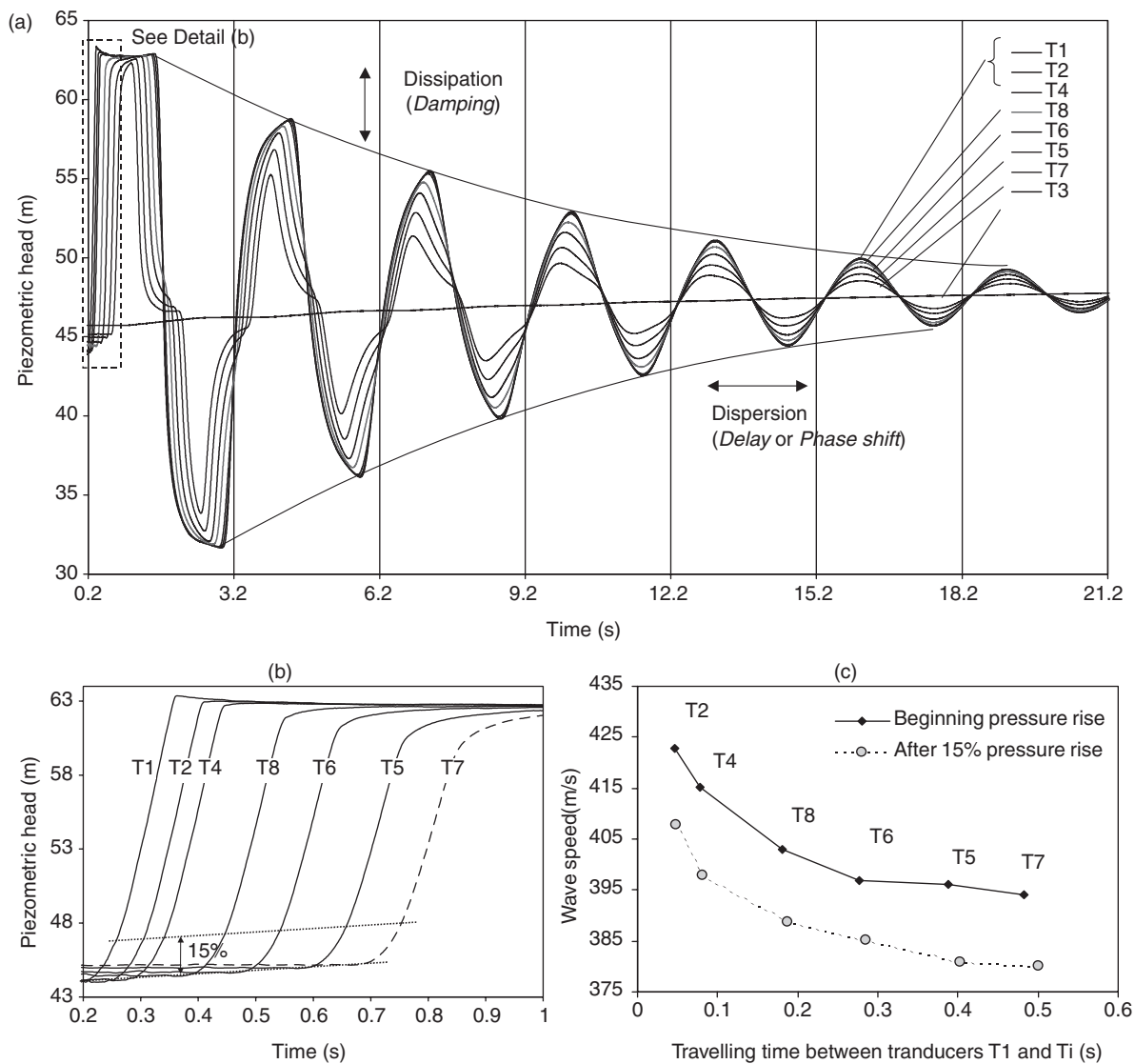


Figure 3 (a) Transient data at eight pressure transducers for valve closure ($Q_0 = 1.01/\text{s}$, $T = 20^\circ\text{C}$). (b) Detail of transient data collected. (c) Wave speed estimation.

mechanical response of polymer materials, particularly PE, and is well known as *viscoelasticity*.

The propagation speed of the pressure wave cannot be estimated by spectral analysis of transient pressure data. The pressure wave disperses considerably in time due to unsteady skin friction, fluid inertial effects and pipe-wall retarded deformation, and frequency analysis simply gives a *rough* estimate of the wave speed. Wave speed in polyethylene pipes is a time-dependent function rather than a constant parameter as it is in linear elastic materials. The initial wave speed, a_0 , was estimated based on the travelling time t^* of the first pressure wave between T1 and the other transducers T_i : $a_0 = L/t^*$, where L is the distance between T1 and T_i . The beginning of the pressure rise and 15% of the total pressure increase were used as the thresholds to compute this time (Fig. 3b). Decreasing wave speeds were obtained with the increase of the transducer distance to the downstream end (Fig. 3c). These wave speeds varied between 423 m/s for T2 (the closest transducer to the downstream end) and 395 m/s for T7 (the furthest), when the beginning of the pressure rise was used. This is because of the continuous delay of the pressure wave with the travelling distance and time. Lower values of the wave speed were observed for 15% of the pressure rise (values between 380 and 410 m/s), as the pressure wave is already slightly delayed.

The same analysis was carried out for the transient event generated with the globe valve opening and for a final steady-state flow of $\sim 0.51/\text{s}$ (Fig. 4). The results are consistent with the previous

ones as the wave speed varied between 390 and 435 m/s. The transient generated by the valve opening dissipates much faster than the one generated by the valve closure.

These values of the wave speed are reference values of the actual elastic wave speed, a_0 , and the dynamic modulus of elasticity of the pipe-wall, E_0 (a_0 of 385 and 425 m/s correspond to E_0 of 1.35 and 1.7 GPa, respectively). Elastic wave speed is an important parameter for the calibration of the mathematical model presented in the companion paper.

2.4 Pressure and circumferential strain time-variation

Transient pressure and strain data for a steady-state flow of 1 l/s, collected in the second set of transient experiments, are presented in Fig. 5. The reference value for the strain (i.e. the zero strain) was considered to be the strain corresponding to the initial steady state conditions, ε_0 . Several observations can be made from the analysis of pressure and circumferential strain time responses.

Once the valve is closed, the maximum overpressure at Location 1 (Transducer T1) decreases slightly and rapidly within the first 0.5 s after the complete valve closure. This is followed by a slight pressure increase until the pressure wave inverts at ~ 1.6 s (Covas *et al.*, 2001, 2002b, 2003b, 2004b). The initial pressure drop is accompanied by a circumferential strain increase. The opposite tendencies of pressure and strain show that the material does not behave in a linear elastic manner in which the strain response has the same trend as the pressure. This is characteristic of viscoelastic behaviour of pipe-wall, as the material stiffens when instantaneously loaded, followed by a retarded stress release with a strain increase and, consequently, a pressure drop. The pressure increases afterwards due to the line packing effect, which is particularly evident at the valve section (Transducer T1). The viscoelastic behaviour of the pipe attenuates the line-packing effect in the first pressure wave, and dissipates it completely in the overall transient pressure signal.

A significant pressure damping is observed in the consecutive pressure waves, which is also characteristic of the pipe-wall retarded deformation. In addition, pressure and strain curves have a particular convex-shape during the loading phase and, the inverse, a concave-shape, during the unloading (pressure release). This is typical of polymer pipe-wall viscoelasticity, given the similarities of the strain curve during loading and unloading phases for a general polymer, and the first pressure and strain waves during the transient event (Covas, 2003). This behaviour significantly influences the pressure response during transients by attenuating the pressure fluctuations in the pipeline and by delaying the pressure wave in time.

2.5 Through-wall strain distribution

Whilst the circumferential strain is measured at the outside wall of the pipe, collected pressure refers to the pressure in the fluid (i.e. at the inner pipe-wall). The pipe has a thick wall with a standard diameter ratio, $SDR = 11$ (SDR is the ratio between the external diameter and the wall thickness). For thick wall pipes, stress and strain distributions cannot be considered uniform throughout

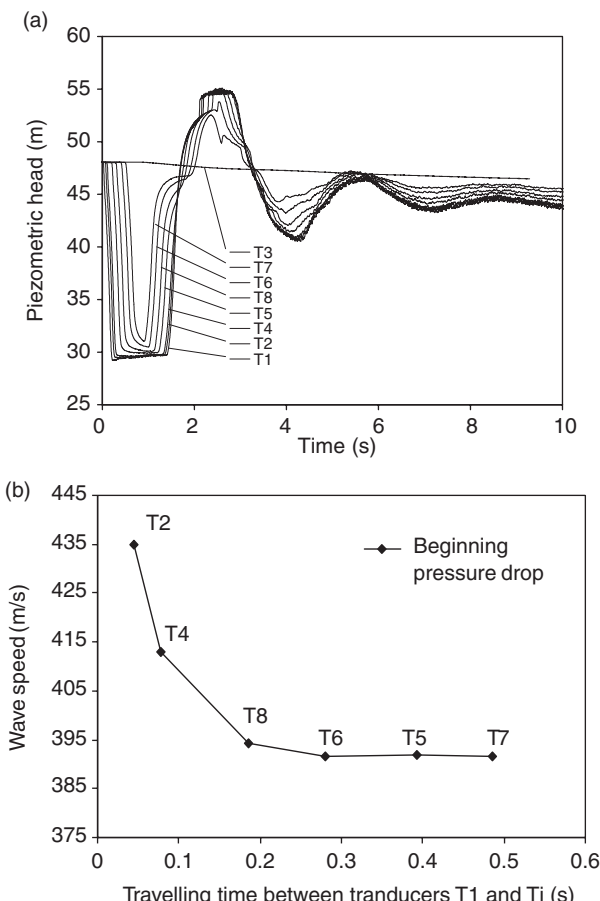


Figure 4 (a) Transient data at eight pressure transducers for valve opening ($Q_{\text{final}} = 0.51/\text{s}$, $T = 20^\circ\text{C}$). (b) Wave speed estimation.

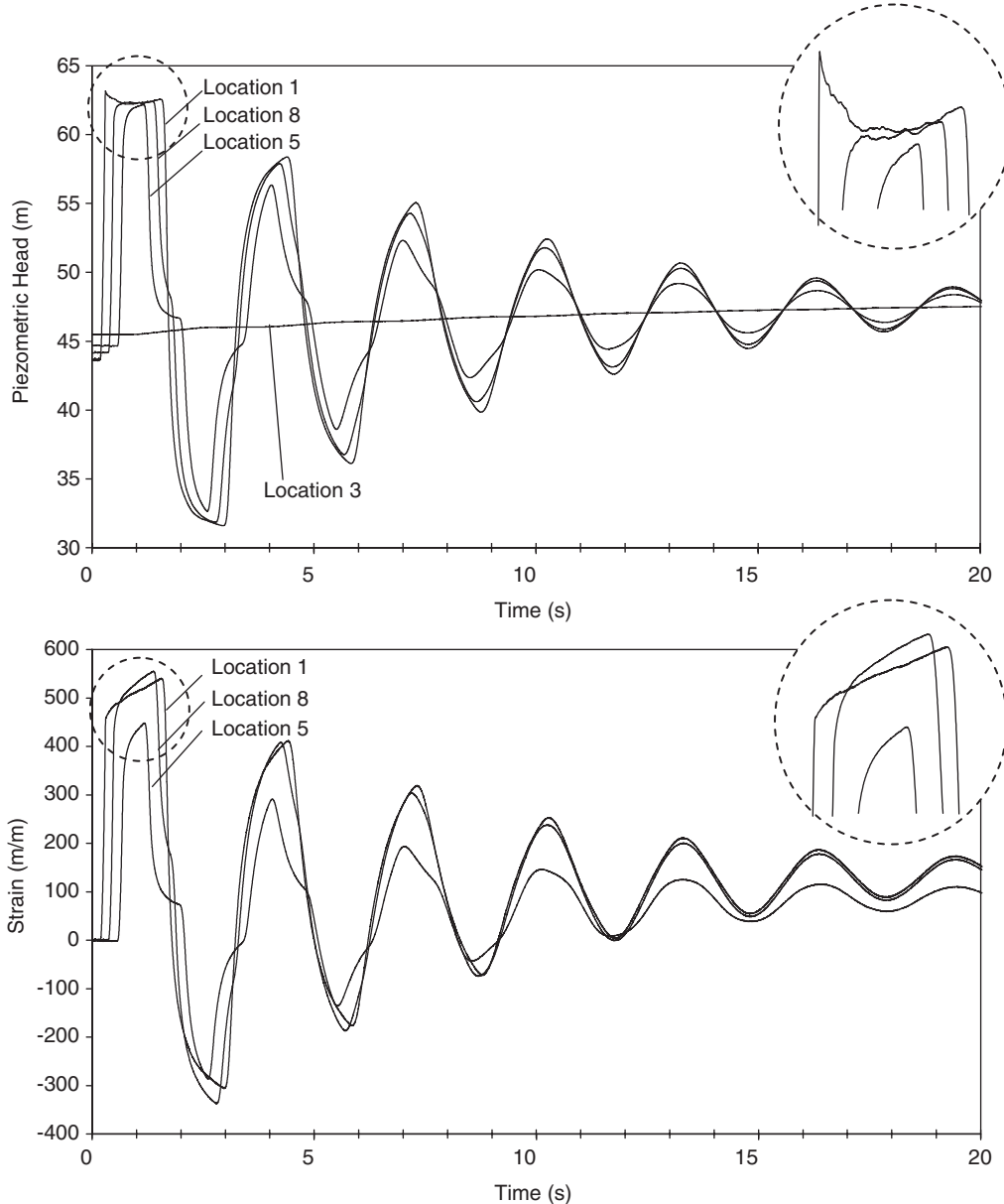


Figure 5 Transient data collected at pressure transducers T3, T5, T8 and T1, and strain gauges SG5, SG8 and SG1 ($Q_0 = 1.01/\text{s}$; $T = 20^\circ\text{C}$).

the wall. Solutions for the displacement and stress fields across the wall are described, in the Theory of Elasticity, by the Lamé Solutions (Westergaard, 1952; Halliwell, 1963; Eringen, 1967; Timoshenko and Goodier, 1970).

For an “infinite linear elastic circular cylindrical tube” subjected to internal and external pressures, p_i and p_o , assuming no movement in the circumferential and axial directions ($u_\theta = u_z = 0$), the radial displacement distribution, u_r , throughout the pipe-wall is (Eringen, 1967):

$$u_r(r) = \frac{a^2 p_i}{2(b^2 - a^2)} \left(\frac{r}{\lambda + \mu} + \frac{b^2}{\mu r} \right) - \frac{b^2 p_o}{2(b^2 - a^2)} \left(\frac{r}{\lambda + \mu} + \frac{a^2}{\mu r} \right) \quad (1)$$

where a and b are inner and outer radii, respectively; r is the generic radius; μ and λ are constants defined for “isotropic

linear-elastic materials” by:

$$\lambda = \frac{E_0 \nu}{(1 + \nu)(1 - 2\nu)} \quad \text{and} \quad \mu = \frac{E_0}{(1 - 2\nu)} \quad (2)$$

where ν is Poisson’s ratio and E_0 is Young’s modulus of elasticity.

For “isotropic linear viscoelastic materials”, the displacement and the stress fields are described by the same expressions as for the elastic case, providing that the elastic constants μ and λ are replaced by the respective viscoelastic functions $\mu(t)$ and $\lambda(t)$, and Young’s modulus of elasticity is replaced by the inverse of the creep compliance function, $1/J(t)$ (Eringen, 1967).

For both cases, the circumferential strain field is given by (Moore and Fuping Hu, 1996):

$$\varepsilon(r) = \frac{r - r_0}{r_0} = \frac{u_r(r)}{r} \quad (3)$$

where r_0 and r are initial and final radii of the pipe, respectively.

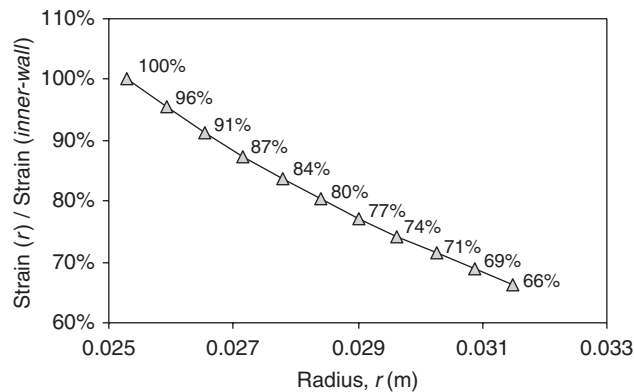


Figure 6 Radial strain field in the pipe-wall expressed in terms of the ratio between the strain for radius r and the strain at the inner pipe wall.

In the current case, the external pressure is zero, the inner pipe diameter $2a$ is 0.0506 m, the outer diameter $2b$ is 0.063 m, and Poisson's ratio ν is 0.46 (given by the manufacturer). Circumferential strain distribution in the pipe-wall obtained by Eq. (3) using (1) and (2) is presented in Fig. 6. This strain field is expressed in terms of maximum strain which corresponds to the strain in the inside wall of the pipe, $r = a$. The strain variation across the wall is not linear, though a linear assumption would be acceptable. The ratio outside/inside strain in the pipe-wall, R_o , is 66%. This ratio will be useful to convert measured outer strain into the strain at the inner pipe-wall. Gally *et al.* (1979) neglected this ratio and thought that observed differences between measured and calculated strains were due to pipe constraints.

Simplified formulae are usually used to calculate the hoop stress at the inner pipe-wall, σ_i , when the outside pressure is null (Chaudhry, 1987; Wylie and Streeter, 1993; Janson, 1995):

$$\sigma_i = \alpha \frac{p_i D}{2e} \quad (4)$$

where D is the pipe internal diameter, e the pipe-wall thickness, p_i the internal pressure, α the dimensionless parameter that takes into account pipe cross-section dimensions and constraints. This formula allows the estimation of the circumferential strain, ε_i , for linear-elastic ($\varepsilon = \sigma/E_0$) and for linear-viscoelastic ($\varepsilon = \sigma J$, where J is the creep function) pipes, respectively, by:

$$\varepsilon_i = \alpha \frac{p_i D}{2eE_0} \quad \text{and} \quad \varepsilon_i = \alpha \frac{p_i D J}{2e} \quad (5)$$

For a "thick wall pipe ($D/e < 25$) anchored along its length", α is (Wylie and Streeter, 1993):

$$\alpha = \frac{2e}{D}(1 + \nu) + \frac{D}{D + e}(1 - \nu^2) \quad (6)$$

The result of Eq. (5) using (6) corresponds exactly to the strain in the interior of the pipe obtained by Eq. (3) using (1) for $r = a$. This is because a pipe anchored along its length is physically equivalent to an infinite hollow cylinder, as both have null axial and hoop displacements.

2.6 Transient mechanical hysteresis

Mechanical hysteresis is usually manifested by a deformation that "lags behind" an applied load. Hysteresis is also observed

when there is more than one strain, for the same stress. Polymers and, surprisingly, metal and other crystalline materials at elevated temperatures or if they are subjected to rapidly varying loads, present a hysteretic behaviour. *Anelasticity* is the term used to describe the hysteretic behaviour of metals (Courtney, 2000).

Collected pressure and circumferential strain data were used to analyse the mechanical hysteresis of the PE pipe. Stress and strain curves were plotted during the transient event (Figs 7 and 8). Circumferential stress at the inner pipe-wall, σ_i , was calculated based on the transient pressure increase, $p_i = p - p_0$, in respect to the steady-state pressure p_0 , by Eqs (4) and (6). Circumferential strain was computed at the inner pipe-wall, ε_i , by correcting the strain with the ratio of outside/inside strain, R_o . Figure 7(a) presents six shots of the time evolution of the stress-strain curve during a transient event. Each of these corresponds to time interval specified in the pressure-time and the strain-time signals in Fig. 7(b).

The mechanical hysteresis of the PE pipe is clear from the analysis of Figs 7 and 8. Stress remains almost constant, whilst strain increases between $t = 1.6$ and 3 s. If the material were linear elastic, strain would remain constant for a constant load. During the inversion of the first pressure wave (between $t = 1.6$ and 3 s), when pressure drops, the stress-strain curve follows a different path from the same curve when the pressure increased. These phenomena are repeated for every loading and unloading phase of the pressure wave. However, stress-strain curves shift around a straight line whose slope corresponds approximately to the average static modulus of elasticity of the pipe, 0.93 GPa (Fig. 8). Although the stress-strain curve starts at zero, the best-fitted straight line ($y = 9.3E + 08x - 3.7E + 04$, where y is the stress and x the strain) does not pass through zero (Fig. 8). This is characteristic of the delayed deformation of the pipe, in which immediately after the stress being removed the material needs time to completely recover.

3 Creep characterization

3.1 Introduction

The simplest description of the viscoelastic behaviour may be achieved by combining the mechanical properties of the linear elastic solid following Hooke's law ($\sigma_0 = E_0 \varepsilon_0$) with the viscous liquid following Newton's law ($\sigma_0 = \eta \partial \varepsilon / \partial t$). Polymers are typically viscoelastic. This behaviour is usually characterized by an instantaneous elastic strain ε_0 followed by a gradual retarded strain $\varepsilon_r(t)$, for an applied load σ_0 . *Creep* is the term used to refer this time-dependent strain behaviour resulting from a constant loading. Creep depends on the molecular structure of the material, temperature and stress-time history. The *creep compliance* $J(t)$ is a function that characterizes this behaviour. By definition, the creep function describes the time-variation of strain, for a constant stress σ_0 , $J(t) = \varepsilon(t)/\sigma_0$. This function can be estimated by a simple creep test or by dynamic testing over a certain range of loading frequencies.

In the current research, the creep compliance function of the PE pipe was estimated by running creep tests in longitudinal

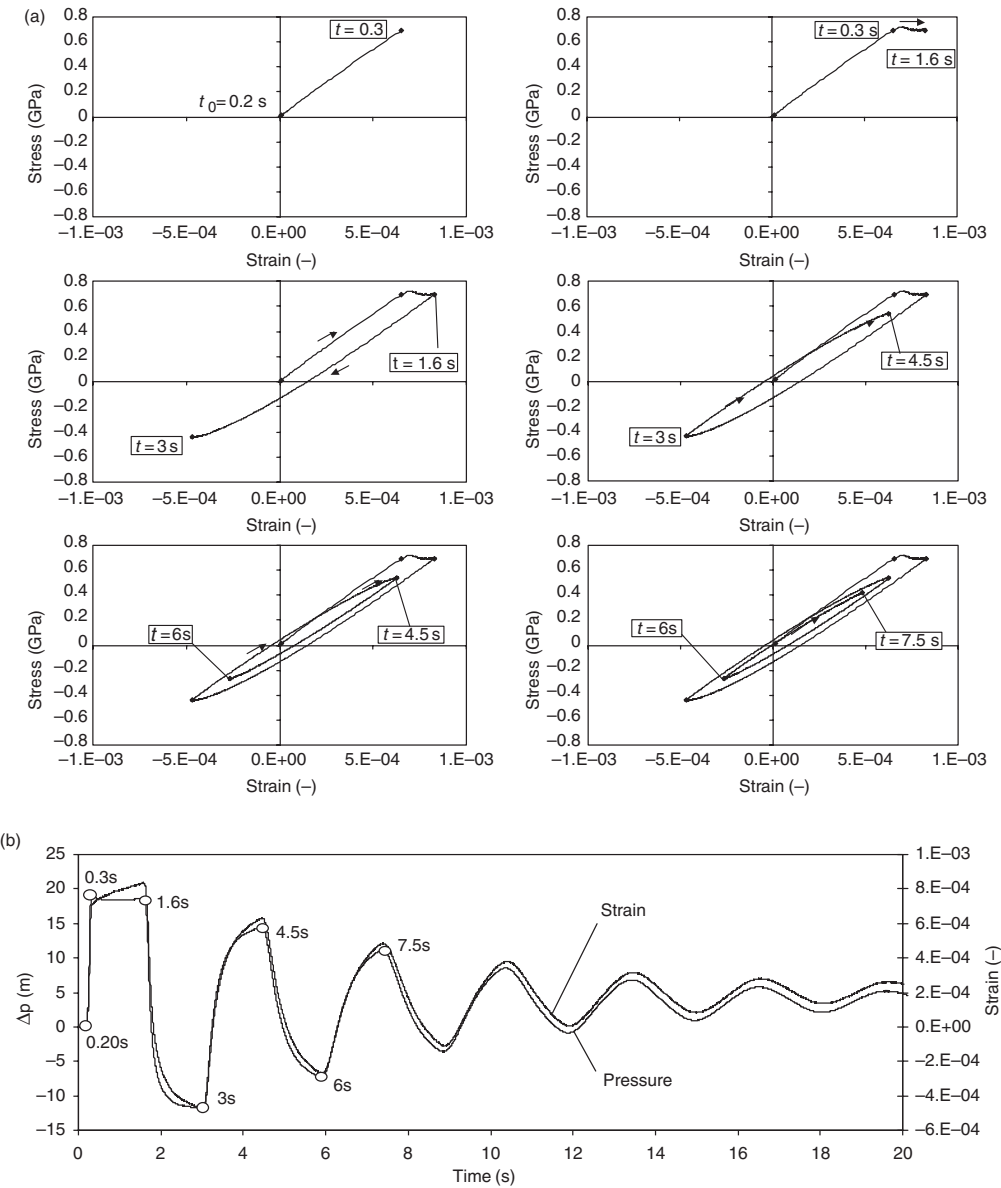


Figure 7 (a) The evolution of stress–strain curves (six plots on the top). (b) Piezometric head and circumferential-strain time variation at Location 1 ($Q_0 = 1.01/\text{s}$; $T = 20^\circ\text{C}$).

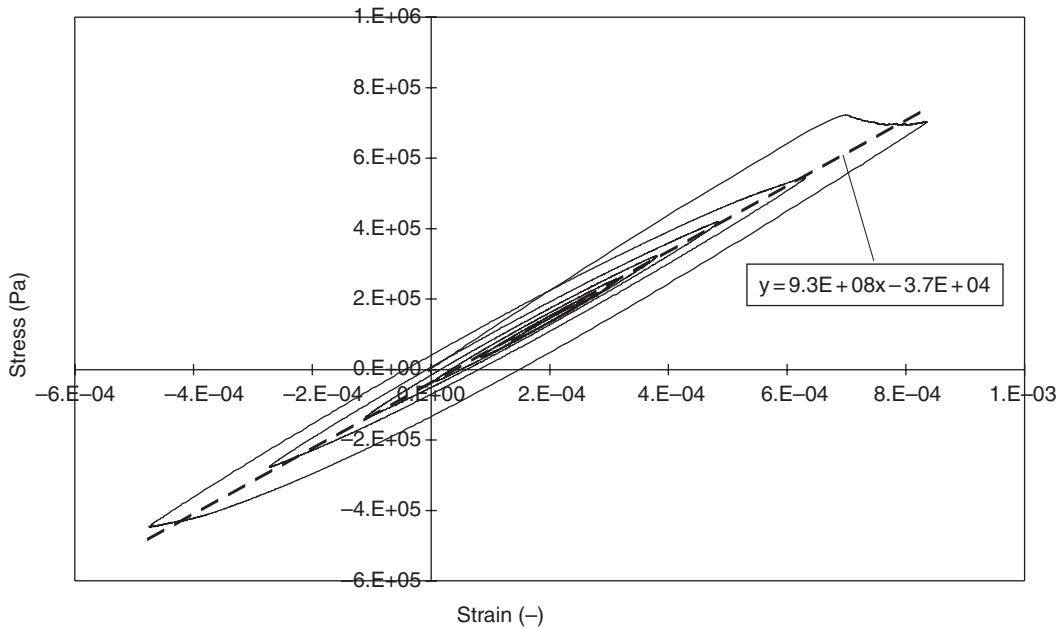


Figure 8 Stress–strain curve during 20 s of transient at Location 1 ($Q_0 = 1.01/\text{s}$; $T = 20^\circ\text{C}$).

samples of pipe. The material was assumed homogenous and isotropic. Two sets of creep tests were run. The first set of creep tests (*Set I*) was carried out at Minho University (MU) and the second one (*Set II*) at Imperial College (IC). Additionally, dynamic mechanical tests were carried at MU to better characterize the viscoelastic properties of the material in terms of molecular structure. The order-of-magnitude of the creep function was also estimated based on pressure and strain data collected directly in the pipe-rig.

3.2 Creep tests

The first set of creep tests (*Set I*) was carried out at the Department of Polymer Engineering, Minho University (Guimarães, Portugal). A DMA7e Perkin-Elmer analyser with a controlled cooling device was used to run these tests. A continuous flux of high purity helium (flow rate of $\sim 28 \text{ cm}^3/\text{min}^{-1}$) was used to improve heat transfer throughout the sample surroundings during the experiments. Pipe samples had a rectangular section (typically $0.7 \times 3 \text{ mm}^2$) and a length of $\sim 20 \text{ mm}$. These samples were cut in the longitudinal direction of the pipe using a diamond saw (Well 3242). Specimens were tested using the tensile mode of the apparatus. Short time creep experiments (15 min) were run for different temperatures from 0 to 25°C . A static stress σ_0 of 1 MPa was used for all these tests. Measured creep data at different temperatures are presented in Fig. 9. The typical instantaneous elastic response (ε_0) followed by a clear viscoelastic trend ($\varepsilon_r(t)$) can be observed. This figure shows the influence of temperature on creep with creep significantly increasing with the temperature. For instance, the creep curve for $T = 25^\circ\text{C}$ is more than twice the curve for $T = 0^\circ\text{C}$. The material becomes more flexible for higher temperatures. This emphasizes the influence and importance of temperature on the creep phenomenon.

The second set of creep tests (*Set II*) was carried out at the Department of Mechanical Engineering, Imperial College (London, UK). The objective was to validate the creep function obtained in the first set of tests and to analyse the influence of the sample cross-section in the stress distribution. An INTRON 5584 machine with 5 kN load cell and accuracy of $\pm 0.5 \text{ N}$ ($\pm 0.01\%$) was used. Samples were cut along the longitudinal direction of

the pipe. Tests were run for samples with different cross-sections (circular and rectangular) and sizes (8, 10, and 15 cm). Very short time creep tests were run (60 min). Temperature was monitored during the tests and was constant at 20°C . Several strain rates were analysed. Creep functions obtained for the strain rate of 0.002 s^{-1} are presented in Fig. 10.

The time-temperature superposition principle was used to obtain a master curve at a reference temperature of $T_{\text{ref}} = 20^\circ\text{C}$ for a larger scale of time for the *Set I* of creep tests. This is particularly important to get a better approximation of the instantaneous component of creep, J_0 . Horizontal shifts along the $\log t$ axis of data were performed until the individual isothermal data formed a single curve. Figure 11(a) shows that a single master curve of the creep data was successfully constructed. This curve describes the time variation of the creep compliance function, $J(t)$, calculated based on the strain between very short times (0.1 s) and long times 1000 s.

Figure 11(b) presents the shift factors associated with the construction of this master curve, $\log a_T$, in an Arrhenius plot. If a thermally activated process is assigned to the viscoelastic features of the material, the shift factors can be parameterised with the Arrhenius equation:

$$\log a_T = \frac{E_a}{R \ln(10)} \left(\frac{1}{T} - \frac{1}{T_{\text{ref}}} \right) \quad (7)$$

A linear relationship is found in the data (Fig. 11b). The activation energy, E_a , obtained from the slope of the Arrhenius fitting, yields 142 kJ/mol. This energy is associated with the energy barrier that the assigned conformational changes within the molecular structure must surpass. The mechanism underlying such motions will influence material creep properties. This can be seen from the large component of viscoelastic response in the total creep curves (Figs 9 and 10), with respect to the instantaneous elastic reaction. Some relaxation process was occurring in the temperature and time-scale of the creep tests. Relaxations, in polymer systems, are usually characterized by a distribution of retardation times, due to the existence of a variety of environments at the molecular level. Total strain can be described by the sum of an elastic and a viscoelastic component. As the viscoelastic component of the creep response is essential in the

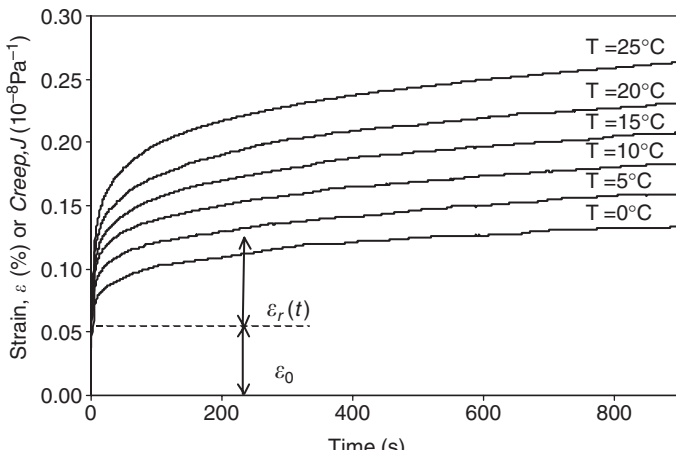


Figure 9 Creep and strain curves at different temperatures (*Set I*).

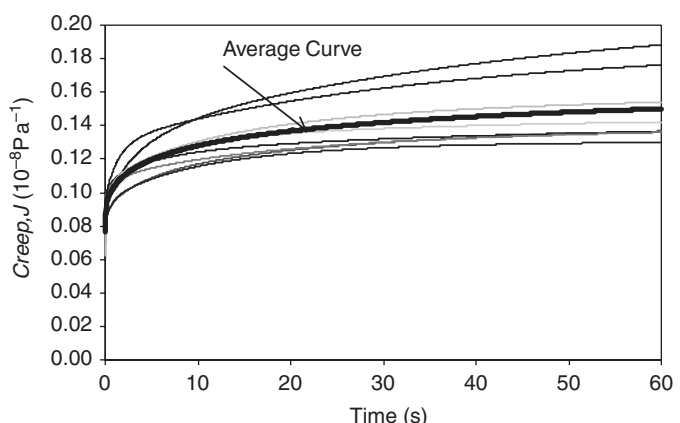


Figure 10 Creep curves for different samples for the strain rate = 0.002 s^{-1} at $T = 20^\circ\text{C}$ (*Set II*).

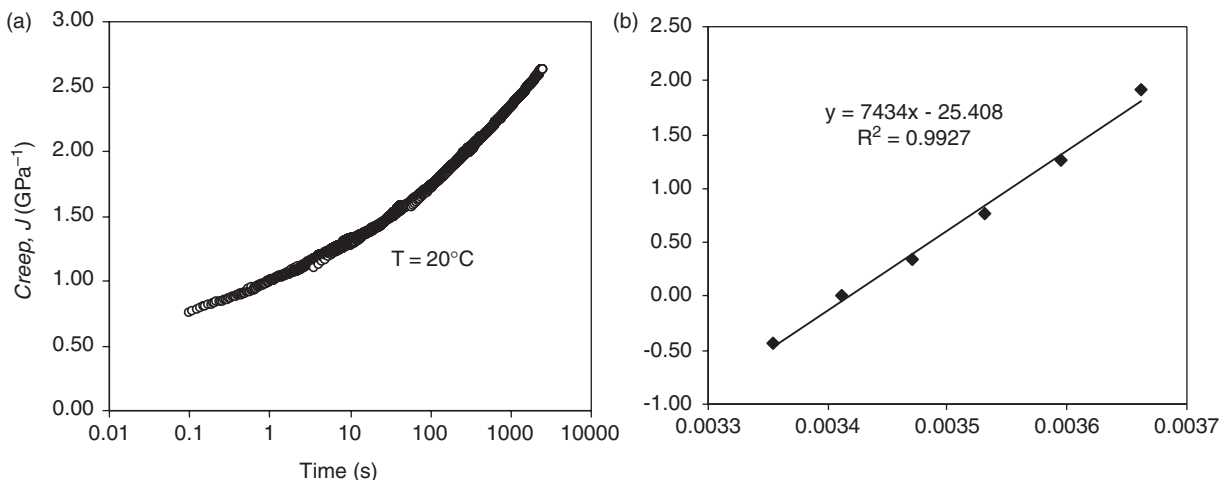


Figure 11 (a) Creep compliance at $T_{\text{ref}} = 20^\circ\text{C}$ obtained by time–temperature superposition (*Set I*), (b) Arrhenius shift factors for $T_{\text{ref}} = 20^\circ\text{C}$. The solid line is the linear fitting of the data.

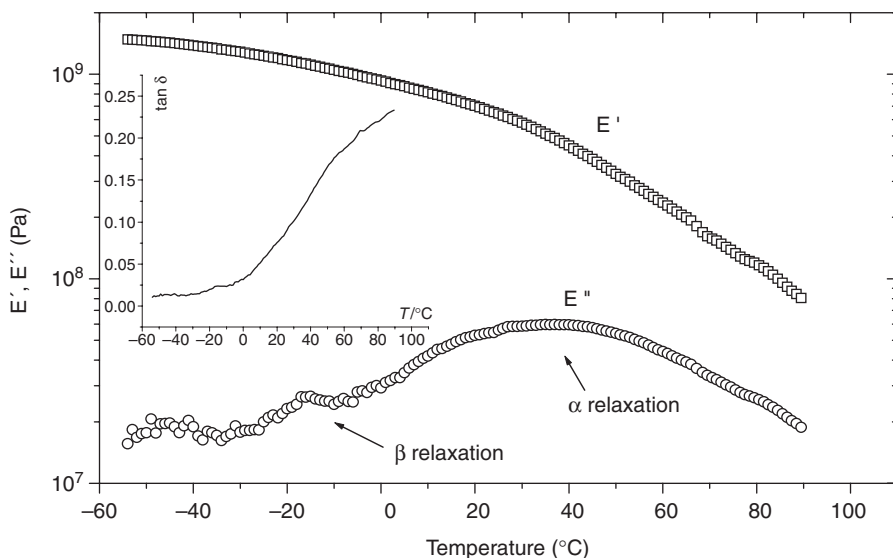


Figure 12 DMA results at 1 Hz, showing the temperature dependence of the storage and loss modulus (E' and E''). The inset graphic shows the variation of the loss factor, $\tan \delta = E''/E'$, with temperature. Both β - and α_c -relaxations are seen in the E'' plot.

modelling of any process depending on the solid-state rheological features of PE, it would be important to understand the origin of molecular motions underlying the relevant relaxation process. Further dynamic mechanical analysis was carried out to provide additional information in this context.

3.3 Dynamic mechanical analysis

Dynamic mechanical analysis (DMA) experiments were carried out using a DMA7e Perkin-Elmer analyser at Minho University to better characterize and understand the viscoelastic properties of the material. Isochronal DMA tests were run for the temperature range approximately -50 to $+90^\circ\text{C}$, at a heating rate of $3^\circ\text{C}/\text{min}$. The dynamic stresses had amplitude of 0.1 MPa and a frequency f of 1 Hz. A static (constant) stress σ_0 of 0.12 MPa was imposed over this dynamic stress.

When a specimen is subjected to a sinusoidal stress, $\sigma = \sigma_0 e^{i\omega t}$, with a rate defined by a frequency f (cycles/s, or Hz) or $\omega = 2\pi f$ (rad/s) and σ_0 being the stress amplitude and

$i = (-1)^{1/2}$, the strain response, though sinusoidal, is neither exactly in phase with the stress (as it would be for the case for a perfectly elastic solid) nor $\pi/2$ out of phase (as it would be for a perfectly viscous fluid). The strain lags behind the stress by some phase angle δ , between 0 and $\pi/2$, $\varepsilon = \varepsilon_0 \exp(i\omega t - \delta)$, where ε_0 is the amplitude of the strain. A full description of the linear viscoelastic response may be provided, for example, by the complex modulus, $E^*(\omega)$, defined as:

$$\begin{aligned} E^*(\omega) &= \frac{\sigma}{\varepsilon} = (\sigma_0/\varepsilon_0) \exp(i\delta) = (\sigma_0/\varepsilon_0)(\cos \delta + i \sin \delta) \\ &= E' + iE'' \end{aligned} \quad (8)$$

The storage modulus, E' , is the elastic (*real*) component of E^* , which is in phase with σ . The loss modulus, E'' , is the viscous (*imaginary*) component of E^* which is $\pi/2$ out of phase with σ .

In the current analysis, both E' and E'' were monitored against temperature for a fixed frequency f of 1 Hz (Fig. 12). Two relaxation processes can be seen in this figure, represented by peaks in the E'' plot. The attribution of different relaxations in PE has been extensively investigated in the past (Boyd, 1985; Mano *et al.*,

2001; and references cited therein). The process at approximately -20°C is the β -relaxation that has been attributed to the glass transition of PE, i.e. to the segmental motions within the amorphous fraction of the material (Boyd, 1985). The low amplitude of this relaxation is related to the high crystalline degree of HDPE. The higher relaxation process centred at approximately 40°C is the α_c -relaxation that has been assigned to screw-like motions within the crystalline component of PE. Such motions should also involve conformational changes in the amorphous regions (Mano, 2001). The values of α_c -relaxation's activation energies scatters strongly in different studies. Typical energies vary from 100 to values higher than 200 kJ/mol (Mano *et al.*, 2001). The obtained activation energy, 142 kJ/mol, is within this interval. It is noted, from Fig. 12, that the α_c -relaxation covers a broad temperature range, including the temperatures at which the creep properties are investigated. This relaxation process is the main "source" of the viscoelastic nature of the analysed polyethylene.

3.4 On-site measurements

Collected transient pressure and strain data were used to compute the creep function in the first 1.6 s, after the transient being generated, assuming a constant overpressure. This provides an order-of-magnitude of the creep function for the on-site conditions, rather than an exact function. Circumferential stresses at the inner pipe-wall were calculated based on collected transient pressure data, by means of Eqs (4) and (6), assuming $p_i = p - p_0$ and the respective physical characteristics of the pipe ($D = 0.0506 \text{ m}$; $e = 0.00625 \text{ m}$; $\nu = 0.46$). Circumferential strain at the inner pipe-wall was calculated based on measured strains using the results of the *Lamé Solution* (ratio outer/inner strain = R_ω). Both stress and strain are expressed as variations towards the steady-state conditions, which is consistent with the linear viscoelasticity assumption. This is not the accurate definition of creep function, as, theoretically, the reference values ε_0 and σ_0 , corresponding to $t = 0 \text{ s}$, should be zero. However, the approximate creep function was computed by:

$$J(t) = \frac{\varepsilon(t)}{\sigma_0} \approx \frac{R_\omega(\varepsilon - \varepsilon_0)}{\frac{\alpha D \gamma}{2e}(\sigma - \sigma_0)} \quad (9)$$

Figure 13 presents creep functions for the transient tests (corresponding to the closure of the globe valve) for different initial flow rates ($Q_0 = 0.054\text{--}1.98 \text{ l/s}$). Creep functions were computed by Eq. (9) and data collected at Location 1. Temperature was monitored in water and in air, being $20 \pm 1^{\circ}\text{C}$. Creep functions estimated using on-site measurements at Location 1 agree fairly well with each other for every different flow condition. Creep functions experimentally determined by the creep tests, Sets I and II, for $T = 20^{\circ}\text{C}$, are represented as well in Fig. 13, and these agree well with the curves obtained based on the stress-strain measurements directly in the pipe-rig.

4 Results and discussion

In general, a good agreement between the creep functions obtained experimentally in mechanical tests and based on pressure and strain direct measurements in the pipe-rig has been observed (Fig. 13). However, in none of these creep tests (*Sets I and II*) was it possible to obtain a good definition of the creep function for very short times (less than 2–3 s), nor the exact value of the elastic creep component, J_0 . Thus, these will have to be calibrated based on the numerical simulation of the fluid system using the transient solver developed in the *companion paper*. Figure 14 presents the creep curves obtained from the mechanical tests (*Sets I and II*) and the model based calibration (Covas *et al.*, 2004a). The model calibration was carried out for laminar flow conditions taking into account unsteady friction by Trikha's formulation (Trikha, 1975). The calibrated curve is slightly lower than any of the experimental curves for $t < 7 \text{ s}$, while for higher times it is within the two curves (*Sets I and II*).

Creep functions obtained by mechanical tests are important for the characterization of the viscoelastic behaviour of PE as a pipe material, providing a good indication of the actual properties of the pipe material. However, these do not correspond exactly to the

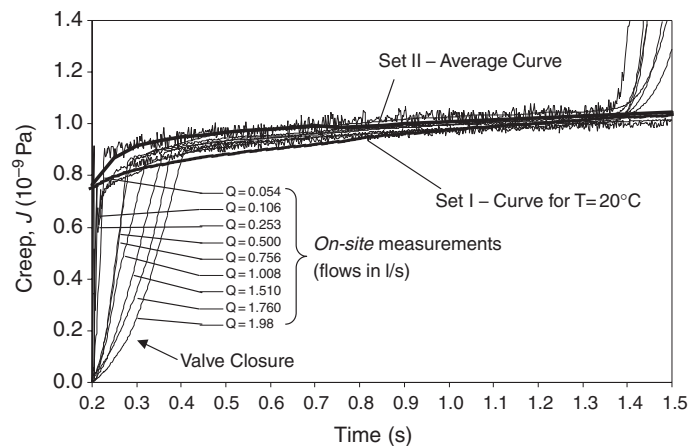


Figure 13 Creep functions based on *on-site* measurements versus creep tests (*Sets I and II*).

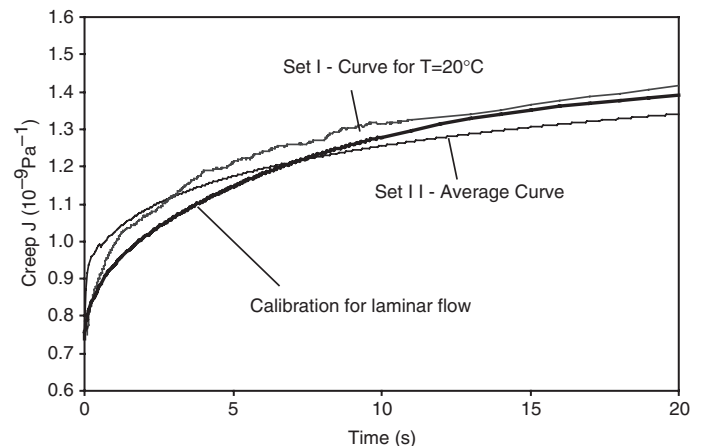


Figure 14 Comparison of creep functions obtained by creep tests (*Sets I and II*) and by calibration for laminar conditions (in the companion paper).

exact creep function of the PE, when integrated in a pipe system, particularly for buried pipes. This is because mechanical tests cannot account for: (i) the variability of material properties; (ii) a slight anisotropy of the pipe; (iii) the increase of pipe stiffness due to axial constraints; and (iv) loading frequency and pipe relaxation.

4.1 Variability of material properties

The measured material properties are not exact quantities. There is always some scatter or variability in data collected from different specimens of the same material. A number of factors lead to uncertainties in measured data. These include the test method, variation in the specimens' fabrication, operator bias and apparatus calibration. Non-homogeneities may exist in the same lot of material and from lot to lot. Temperature is another parameter on which creep depends and it is extremely sensitive. A slight temperature variation may significantly change the creep response. The accuracy of the equipment used to run the tests is another important factor.

4.2 Residual stress and anisotropy

The residual stress in an isotropic thermoplastic plastic pipe is an inherent characteristic of the conventional manufacturing process via melt extrusion and subsequent rapid cooling (Janson, 1995; Clutton and Williams, 1995; Kazakov, 1998). The constraint in thermal contraction during solidification yields a through-wall resultant hoop stress being formed due to a differential cooling. The magnitude of the residual stresses is determined by the shear stress developed inside the die as well as by the rate of cooling (Hodgkinson and Williams, 1983). This results in anisotropy and non-homogeneity in the material. Zhang and Moore (1997) analysed the pipe anisotropy in samples of a thick wall extruded HDPE pipe, cut in the three directions of the pipe (longitudinal, radial and circumferential). This HDPE pipe was isotropic in the circumferential and longitudinal directions, and presented a small degree of anisotropy in the radial direction for strains higher than 5%.

4.3 Pipe constraints

The mechanical behaviour of the PE pipe system is dependent on the stiffness of the surrounding environment and the pipe physical constraints (Zhang and Moore, 1997). Larson and Jonsson (1991) analysed the elastic properties of a PVC pipeline, in the field, under buried and unburied conditions, during transient events. The soil surrounding the pipe decreased the circumferential strain and increased the pressure, acting as an external support and increasing the pipe modulus of elasticity from 2.9 to 6.8 GPa. Ivankovic and Vinizelos (1998) analysed the crack propagation in a plastic pipe unburied and buried under gravel. The gravel backfill increased the overall pipe mechanical resistance, increasing the pipe crack pressure by 40% and reducing the crack propagation speed by 30%. Similarly, the mechanical behaviour of PE in the pipe-rig, though unburied, relies upon the axial and radial constraints of the pipe and connection fittings.

4.4 Loading frequency and pipe relaxation

The pipe material has a linear viscoelastic behaviour for the range of strains of transient events generated (maximum strains = 0.3%). HDPE presents a non-linear viscoelastic behaviour only at high strain levels (strains > 5%) (Zhang and Moore, 1997). However, transient tests were run systematically and repeatedly. After 1 day of tests, the pipe material presented a residual strain (relaxation) for a null load. This was a result of not allowing the material enough time to recover after so many loading and unloading processes. This situation was partially reproduced during the Imperial College creep tests, as the same sample was repeatedly loaded and unloaded. The results of the creep tests for a sequence of three creep tests are presented in Fig. 15. Although linear viscoelastic, PE behaviour depends on the past time history of loads and pipe relaxations. After creep tests and not by allowing enough time for recovery, the PE sample is relaxed and when a new test is run, the creep tends to come back to the initial creep curve (Fig. 15b). If creep functions are estimated by Eq. (9), these tend to decrease and to have a lower slope with the number of tests (Fig. 15a). If creep functions are calculated by the ratio strain/stress, the relaxation of the material can be observed by the increase of creep curves (Fig. 15c).

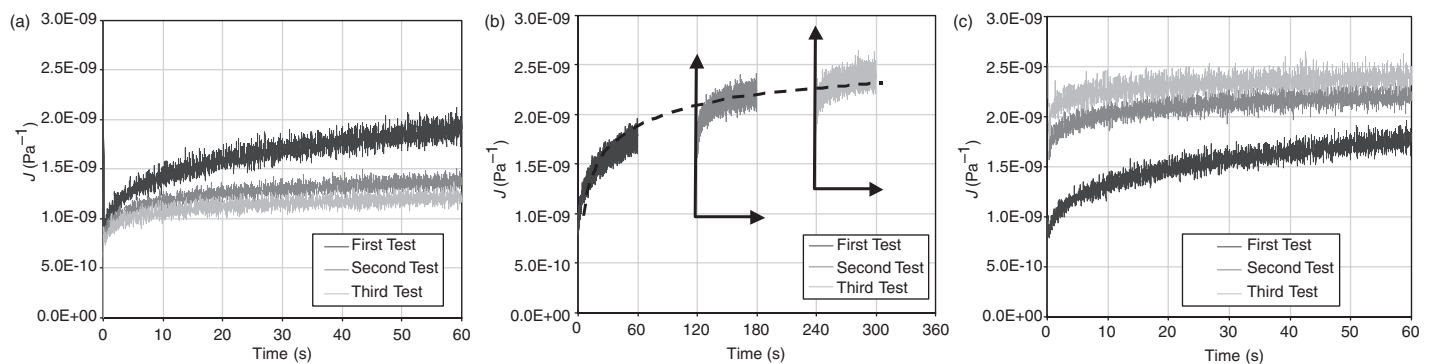


Figure 15 Set II of Creep functions (*not filtered*): (a) calculated by Eq. 9; (b) calculated by $J = \varepsilon/\sigma$ and plotted in real time and (c) calculated by $J = \varepsilon/\sigma$.

Summarizing, the creep function can be determined experimentally for each material and temperature, though it may not represent the accurate mechanical behaviour of the material in the pipe system. This is not only due to the variability of material properties and anisotropy, but also because pipe-creep depends on the stress time-history of the pipe (namely on the loading frequency and amplitude) and the axial and circumferential constraints of the system (a buried pipe does not have the same response as an unburied pipe). As $J(t)$ of the material is known, the effect of the stress time-history could be taken into account in the simulation of ε using the Boltzmann-superposition principle, providing that the stress-history is identified. The creep compliance is a function with several sources of uncertainty. In a design stage, creep data given by manufacturers or determined for similar materials can be used. In an existing system, pressure data should be collected and creep should be calibrated using an adequate transient solver and these data, rather than relying on creep or dynamic testing of the pipe material.

5 Summary and conclusions

The dynamic effect of the pipe-wall viscoelasticity in hydraulic transients has been analysed based on transient data collected from a HDPE pipe-rig at Imperial College. The retarded deformation of the pipe-wall causes the mechanical damping of the transient pressure wave. The pressure wave is highly attenuated and dispersed in time. A sudden pressure drop occurs immediately after the fast valve closure. Mechanical hysteresis of the pipe material is observed during the transient event, based on the analysis of transient pressure and strain data. These are typical of the viscoelastic mechanical behaviour of polymers, particularly of PE. Overpressures estimated assuming a linear elastic mechanical behaviour of the pipe can be under estimated in 5–25% in PE pipes, which is an important reason for taking into account this behaviour.

Viscoelastic mechanical behaviour is usually characterized by a creep function. This function was determined experimentally by two sets of tests. Variability in the results was observed which is expected for this type of material. The creep function was also estimated based on the strain/stress measured ratio directly in the pipe-rig, for the first half-period of the pressure wave. Although creep functions are in the range of expected values, a slight disagreement of these curves is observed. This can be due to the variability of the material properties, pipe anisotropy, on-site pipe constraints and pipe relaxation. The elastic (instantaneous) creep could not be measured in creep tests, though it can be estimated based on the speed propagation of the first pressure wave between transducers.

In conclusion, creep can be measured experimentally for a certain material and temperature. However, this function only provides an approximate curve and trend of the actual pipe response. This is because there are external factors, such as pipe constraints and stress-time history, which cannot be accounted for in these tests. Creep data can be used to analyse hydraulic transients in polymeric pipes during the design stage. When there is

available transient pressure data, the creep should be determined based on the calibration of an adequate viscoelastic transient simulator.

Acknowledgments

The results presented here were achieved through a joint research project between the University of Exeter and Imperial College London supported by the UK Engineering and Physical Sciences Research Council (Inverse Transient Analysis for Pipe Roughness Calibration and Leak Detection). Additionally, Dídia Covas gratefully acknowledges the financial support of Fundação da Ciência e Tecnologia (FCT, Portugal) and Instituto Superior Técnico (IST, Portugal).

Notation

- a = pipe inner diameter (m)
- a_0 = elastic wave speed (m/s)
- a_T = shift factor (–)
- b = pipe outer diameter (m)
- D = pipe internal diameter (m)
- e = pipe-wall thickness (m)
- E^* = complex modulus of elasticity (Pa)
- E' = elastic (or real) component of E^* (Pa)
- E'' = viscous (or imaginary) component of E^* (Pa)
- E_0 = dynamic modulus of elasticity (Pa)
- E_a = activation energy (kJ/mol)
- f = frequency (Hz)
- H_0 = steady-state piezometric head (m)
- J = creep-compliance (Pa^{-1})
- J^* = complex modulus of creep-compliance (Pa)
- J' = the elastic (or real) component of J^* (Pa)
- J'' = the viscous (or imaginary) component of J^* (Pa)
- p = pressure (Pa)
- p_0 = steady-state pressure (Pa)
- p_i = pressure inside the pipe (Pa)
- p_o = pressure outside the pipe (Pa)
- Q_0 = steady-state flow-rate (m/s)
- r, r_0 = pipe radius and initial pipe radius (m)
- R = gas constant (–)
- R_ω = ratio between the outer strain and the inner strain in the pipe-wall (–)
- T = temperature ($^\circ\text{C}$)
- t = time (s)
- T_{ref} = reference temperature ($^\circ\text{C}$)
- u_θ = circumferential displacement of the pipe-wall (m)
- u_r = radial displacement of the pipe-wall (m)
- u_z = axial displacement of the pipe-wall (m)
- α = dimensionless parameter function of the pipe cross-section and constraints (–)
- ν = Poisson's ratio of the pipe (ratio between axial and circumferential strain) (–)
- ε = circumferential strain (–)

- ε_i = circumferential strain at the inner surface of the pipe-wall (—)
 ε_0 = initial strain (—)
 μ, λ = constant associated with Poisson's ratio and modulus of elasticity (Pa)
 ω = angular frequency (rad)
 δ = frequency lag (rad)
 σ_i = hoop stress at the inner surface of the pipe-wall (Pa)
 σ = stress; circumferential-stress (Pa)
 σ_0 = initial stress (Pa)
 τ = retardation time (s)

References

- AKLONIS, J.J., MACKNIGHT, W.J. and SHEN, M. (1972). *Introduction to Polymer Viscoelasticity*. John Wiley & Sons, Inc, New York.
- BOYD, R.H. (1985). "Relaxation Processes in Crystalline Polymers: Experimental Behaviour—A Review". *Polymer* 26, 323–347.
- CHAUDHRY, M.H. (1987). *Applied Hydraulic Transients* 2nd edn. Litton Educational Publishing Inc, Van Nostrand Reinhold Co., New York.
- CLUTTON, E.Q. and WILLIAMS, J.G. (1995). "On the Measurement of Residual Stress in Plastic Pipes". *Polym. Engng. Sci.*, 35(17), 1381–1386.
- COURTNEY, T.H. (2000). *Mechanical Behaviour of Materials*, 2nd edn. McGraw-Hill, New York.
- COVAS, D. (2003). "Inverse Transient Analysis for Leak Detection and Calibration of Water Pipe Systems—Modelling Special Dynamic Effects". PhD Thesis, Imperial College of Science, Technology and Medicine, University of London, London, UK.
- COVAS, D., STOIANOV, I., GRAHAM, N., MAKSIMOVIC, C., RAMOS, H. and BUTLER, D. (2001). "Leakage Detection in Pipelines Systems by Inverse Transient Analysis: From Theory to Practice". In: ULANICKI, B., COULBECK, B. and RANCE, J. (eds), *Water Software Systems: Theory and Applications* Pub. Res. Studies Press, *Proceeding International Conference on Computing and Control for the Water Industry*, CCWI 2001, De Montford University, Leicester, UK, 3–16.
- COVAS, D., STOIANOV, I., BUTLER, D., MAKSIMOVIC, C., GRAHAM, N. and RAMOS, H. (2002a). "Inverse Transient Analysis for Leak Detection and Calibration—A Case Study in a Polyethylene Pipeline". *Proceedings of 5th International Conference on Hydroinformatics*. In: CLUCKIE, I.D., HAN, D., DAVIS, J.P. and HESLOP, S. (eds), IWA, Cardiff, Wales, UK, pp. 1154–1159.
- COVAS, D., STOIANOV, I., GRAHAM, N., MAKSIMOVIC, C., RAMOS, H. and BUTLER, D. (2002b). "Hydraulic Transients in Polyethylene Pipes". *Proceedings of 1st Annual Environmental & Water Resources Systems Analysis (EWRSA) Symposium*, A.S.C.E. EWRI Annual Conference, Roanoke, Virginia, USA (CD-ROM).
- COVAS, D., RAMOS, H., GRAHAM, N., MAKSIMOVIC, C., KAPELAN, Z., SAVIC, D. and WALTERS, G. (2003a). "An Assessment of the Application of Inverse Transient Analysis for Leak Detection: Part II—Collection and Application of Experimental Data". *Proceedings of the International Conference on Computers and Control in the Water Industry* (CCWI 2003), Imperial College London, UK, 15–17 September 2003. Balkema, Rotterdam.
- COVAS, D., STOIANOV, I., MANO, J., RAMOS, H., GRAHAM, N. and MAKSIMOVIC, C. (2004a). "The Dynamic Effect of Pipe-Wall Viscoelasticity in Hydraulic Transients. Part II—Model Development, Calibration and Verification". *J. Hydraul. Res., IAHR* (in press).
- COVAS, D., STOIANOV, I., RAMOS, H., GRAHAM, N. and MAKSIMOVIC, C. (2003b). "The Dissipation of Pressure Surges in Water Pipeline Systems". In: CABRERA and CABRERA Jr. (eds), *First Joint Conference IAHR-IWA on Pumps, Electromechanical Devices and Systems Applied to Urban Water Management* Valencia, Spain. Swets&Zeitlinger, Lisse, pp. 711–719.
- COVAS, D., RAMOS, H., GRAHAM, N. and MAKSIMOVIC, C. (2004b). "The Interaction Between the Viscoelastic Behaviour of the Pipe-Wall, Unsteady Friction and Transient Pressures". *The Practical Application of Surge Analysis for Design and Operation, 9th International Conference on Pressure Surges*, Chester, UK, 24–26 March 2004. BHR Group Ltd., London (to be presented).
- ERINGEN, A.C. (1967). *Mechanics of Continua*. John Wiley & Sons, Inc., New York.
- FERRY, J.D. (1970). *Viscoelastic Properties of Polymers*, (2nd edn). John Wiley & Sons, New York.
- FOX JR., G.L. and STEPNEWSKI, D. (1974). "Pressure Wave Transmission in a Fluid Contained in a Plastically Deforming Pipe". *J. Press. Ves. Technol., Trans. ASME* 258–262.
- FRANKE, G. and SEYLER, F. (1983). "Computation of Unsteady Pipe Flow with Respect to Viscoelastic Material Properties". *J. Hydraul. Res., IAHR* 21(5), 345–353.
- GALLY, M., GUNAY, M. and RIEUTFORD, E. (1979). "An Investigation of Pressure Transients in Viscoelastic Pipes". *J. Fluid Engng., Trans. ASME* 101, 495–499.
- HALLIWELL, A.R. (1963). "Velocity of Water Hammer Wave in an Elastic Pipe". *J. Hydraul. Div., ASCE* 75(HY4) (2), 1–21.
- HODGKINSON, J.M. and WILLIAMS, J.G. (1983). "The Measurement of Residual Stresses in Plastic Pipes". *Plastics Rubber Process. Appl.* 3(1), 37–42.
- IVANKOVIC, A. and VENIZELOS, G.P. (1998). "Rapid Crack Propagation in Plastic Pipe: Predicting Full-Scale Critical Pressure from S4 Test Results". *Engng. Fracture Mech.* 59(5), 607–622.
- JANSON, L.-E. (1995). *Plastics Pipes for Water Supply and Sewage Disposal*, Borealis, Stockholm.
- KAZAKOV, A. (1998). "An Automated Method for the Measurement of Residual Stress in Melt-Extruded Plastic Pipes". *Polym. Testing* 17, 443–450.

24. LARSON, M. and JONSSON, L. (1991). "Elastic Properties of Pipe Materials During Hydraulic Transients". *J. Hydraul. Engng., ASCE* 117(10), 1317–1331.
25. MANO, J. (2001). "Cooperativity in the Crystalline Alpha-Relaxation in Polyethylene". *Macromolecules* 34, 8825–8828.
26. MANO, J., SOUSA, R.A., REIS, R.L., CUNHA, A.M. and BEVIS, M.J. (2001). "Viscoelastic Behaviour and Time-Temperature Correspondence of HDPE with Varying Levels of Processinduced Orientation". *Polymer* 42, 6187–6198.
27. MEIBNER, E. and FRANKE, G. (1977). "Influence of Pipe Material on the Dampening of Waterhammer". *Proceedings of the 17th Congress of the International Association for Hydraulic Research*. IAHR, Baden-Baden, Germany.
28. MITOSEK, M. and ROSZKOWSKI, A. (1998). "Empirical Study of Waterhammer in Plastic Pipes". *Plastics, Rubber Composites Process Appl.* 27(7), 436–439.
29. MOORE, I.D. and FUPING HU (1996). "Linear Viscoelastic Modelling of Profile High Density Polyethylene". *Can. J. Civil Engng.* 23(395), 407.
30. RAMOS, H., BORGES, A., COVAS, D. and LOUREIRO, D. (2004). "Surge Damping Analysis in Pipe Systems: Modelling and Experiments". *J. Hydraul. Res., IAHR* (in press).
31. RIANDE, E., DÍAZ-CALLEJA, R., PROLONGO, M.G., MASEGOSA, R.M. and SALOM, C. (2000). *Polymer Viscoelasticity: Stress and Strain in Practice*. Marcel Dekker, Inc., New York.
32. RIEUTFORD, E. (1982). "Transients Response of Fluid Viscoelastic Lines". *J. Fluid Engng., ASME* 104, 335–341.
33. RIEUTFORD, E. and BLANCHARD, A. (1979). "Ecoulement Non-permanent en Conduite Viscoelastique—Coup de Bélier". *J. Hydraul. Res., IAHR* 17(1), 217–229.
34. STOIANOV, I., KARNEY, B., COVAS, D., MAKSIMOVIC, C. and GRAHAM, N. (2002). "Wavelet Processing of Transient Signals for Pipeline Leak Location and Quantification". *Proceedings of 1st Annual Environmental & Water Resources Systems Analysis (EWRSA) Symposium, A.S.C.E. EWRI Annual Conference*, Roanoke, Virginia, USA (CD-ROM).
35. SUO, L. and WYLIE, E.B. (1990). "Complex Wave Speed and Hydraulic Transients in Viscoelastic Pipes". *J. Fluid Engng., Trans. ASME* 112, 496–500.
36. TIMOSHENKO, S.P. and GOODIER, J.N. (1970). *Theory of Elasticity*. McGraw-Hill Book Co., New York.
37. TRIKHA, A.K. (1975). "An Efficient Method for Simulating Frequency-Dependent Friction in Transient Liquid Flow". *J. Fluids Engng., Trans. ASME* 97(1), 97–105.
38. WESTERGAARD, H.M. (1952). *Theory of Elasticity and Plasticity*. John Wiley & Sons, Inc. and Harvard University Press, New York, and Bastor.
39. WILLIAMS, D.J. (1977). "Waterhammer in Non-Rigid Pipes: Precursor Waves and Mechanical Dampening". *J. Mech. Engng., ASME* 19(6), 237–242.
40. WYLIE, E.B. and STREETER, V.L. (1993). *Fluid Transients in Systems*. Prentice Hall, Englewood Cliffs, NJ.
41. ZHANG, C. and MOORE, I.D. (1997). "Non-Linear Mechanical Response of High Density Polyethylene. Part I: Experimental Investigation and Model Evaluation". *Polym. Engng., Sci.* 37(2), 404–413.